

# SURFACE SOLAR ULTRAVIOLET RADIATION FOR PALEOATMOSPHERIC LEVELS OF OXYGEN AND OZONE

JOEL S. LEVINE

*Atmospheric Environmental Sciences Division, NASA Langley Research Center, Hampton  
Va. 23665, U.S.A.*

(Received 7 April; in revised form 11 August, 1980)

**Abstract.** Many investigators have concluded that the level of solar ultraviolet radiation (200–300 nm) reaching the surface was a key parameter in the origin and evolution of life on Earth. The level of solar ultraviolet radiation between 200 and 300 nm is controlled primarily by molecular absorption by ozone, whose presence is strongly coupled to the level of molecular oxygen. In this paper, we present a series of calculations of the solar ultraviolet radiation reaching the surface for oxygen levels ranging from  $10^{-4}$  present atmospheric level to the present level. The solar spectrum between 200 and 300 nm has been divided into 34 spectral intervals. For each spectral interval, we have calculated the solar ultraviolet radiation reaching the Earth's surface by considering the attenuation of the incoming beam due to ozone and oxygen absorption. A one-dimensional photochemical model of the atmosphere was used for these calculations.

## 1. Introduction

Life on planet Earth is shielded from lethal solar ultraviolet radiation by a thin layer of stratospheric ozone ( $O_3$ ) located about 25 km above the surface. Ozone strongly absorbs between 200 and 300 nm, and does not permit solar ultraviolet radiation shorter than 300 nm to reach the ground (molecular oxygen,  $O_2$ , strongly absorbs shortward of 200 nm). The maximum cell absorption of solar ultraviolet radiation arises from its absorption by nucleic acids (RNA, DNA) peaking between 250 and 270 nm. Cell absorption of ultraviolet radiation in these bands is highly lethal to all known forms of organized cell activity. While the coincidence may be fortuitous, the maximum in the absorption spectra of nucleic acids coincides with the maximum in the absorption spectra of ozone.

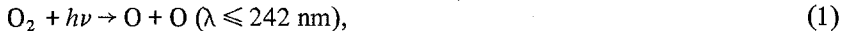
The role of biologically harmful solar ultraviolet radiation on the origin and evolution of life on Earth has been discussed by Berkner and Marshall (1965), Sagan (1973), and Margulis *et al.* (1976). Sagan (1973) has pointed out that unprotected microorganisms at the Earth's surface would be destroyed in a matter of seconds if exposed to solar ultraviolet radiation prior to the appearance of ozone ( $O_3$ ) in the paleoatmosphere. Sagan has also pointed out that an ultraviolet screen could not have been provided by other species in the paleoatmosphere, i.e., methane, ammonia, water vapour, carbon dioxide, nitrogen, hydrogen, or hydrogen sulfide, since none of these gases absorb sufficiently strongly at wavelengths near 240 nm. Berkner and Marshall have speculated that Precambrian life was confined to very restricted habitats by the strong flux of lethal solar ultraviolet that bathed the Earth's surface prior to the development of the ozone layer. The development of the  $O_3$  layer is presumed to have made possible, for the first time, the opening of land

for life, accompanied by diversification of life and the subsequent formation of abundant fossils, according to the scenario of Berkner and Marshall. However, this scenario has recently been questioned by Margulis *et al.* (1976) and Rambler *et al.* (1976).

To study the chronology of the solar ultraviolet radiation reaching the Earth's surface over geological time, two factors must be considered. The first is the calculation of the ultraviolet radiation reaching the surface, as a function of  $O_3$  level, which is a function of the atmospheric  $O_2$  level. The second concerns the exact chronology for the evolution of atmospheric  $O_2$ . The first point in the topic of this paper. The second point is not addressed in this paper, except to point out that at the present time, there is considerable uncertainty concerning the exact chronology for the evolution of  $O_2$  in the Earth's atmosphere, as discussed in Section 3.

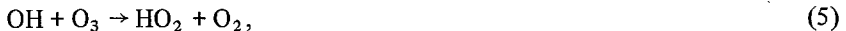
## 2. The Chemistry of Atmospheric Ozone

About 90% of all atmospheric ozone is found in the stratosphere between 15 and 50 km. Our knowledge of the chemistry of ozone has expanded greatly over the last 10 years. The first photochemical model for  $O_3$  was developed by Chapman (1930). Chapman's photochemical model included four reactions, all involving the interconversion of oxygen allotropes (molecular oxygen ( $O_2$ ), atomic oxygen (O), and ozone ( $O_3$ )), but neglected the effects of vertical eddy transport on the distribution of  $O_3$ . Chapman's photochemical scheme included the following reactions:



The energy of solar photons responsible for photodissociation is represented by  $h\nu$ , where  $h$  is Planck's constant and  $\nu$  is the frequency of the photons corresponding to the photodissociation threshold given in parenthesis.

Bates and Nicolet (1950) expanded Chapman's photochemical scheme to include the effects of the odd hydrogen species,  $HO_x$  (H, OH,  $HO_2$ ), on  $O_3$  and O. The odd hydrogen species chemistry includes the following important catalytic cycle for  $O_3$  destruction:



Catalytic reactions (5) and (6) result in the net destruction of both  $O_3$  and O via reaction (4), i.e.,  $O_3 + O \rightarrow 2O_2$ . In addition to the  $HO_x$  catalytic cycle, other  $HO_x$  reactions lead to the destruction of ozone.

The reaction between  $H_2O$  and excited oxygen atoms,  $O(^1D)$ , and the photodissociation of  $H_2O$  are important sources of OH, represented by reactions (7) and (8), respectively.



More recently, Crutzen (1970, 1971) and Johnston (1971) pointed out the importance of nitrogen oxides,  $\text{NO}_x$  ( $\text{NO} + \text{NO}_2$ ), in the destruction of  $\text{O}_3$ .  $\text{O}_3$  is destroyed by  $\text{NO}$  via the  $\text{NO}_x$  catalytic cycle:



Again catalytic reactions (9) and (10) result in the net destruction of both  $\text{O}_3$  and  $\text{O}$  via reaction (4). The major source of stratospheric  $\text{NO}_x$  is the reaction of  $\text{O}({}^1\text{D})$  with  $\text{N}_2\text{O}$ :



$\text{N}_2\text{O}$  is produced biogenically by soil bacteria and diffuses up to the stratosphere where it forms  $\text{NO}$  via reaction (11). Recently, it has been suggested that atmospheric lightning may be an additional previously unsuspected natural source of  $\text{N}_2\text{O}$  (Levine *et al.*, 1979a). It has been estimated that the Chapman loss mechanisms may account for about 20% of the total stratospheric destruction of  $\text{O}_3$ , with  $\text{HO}_x$  chemistry accounting for about 10% and  $\text{NO}_x$  chemistry accounting for about 70% of the total stratospheric destruction of  $\text{O}_3$  (Johnston, 1975).

### 3. The Evolution of Ozone

The appearance and evolution of stratospheric  $\text{O}_3$  over geological time have been investigated by several researchers using photochemical models of increasing complexity. The appearance and evolution of  $\text{O}_3$  were strongly coupled to the appearance and evolution of molecular oxygen ( $\text{O}_2$ ). The chemical evolution of the atmosphere has recently been discussed by Walker (1977) and Hart (1978). The sources of  $\text{O}_2$  in the atmosphere have been reviewed by Berkner and Marshall (1965), Brinkmann (1969), Towe (1978), and Walker (1978). The photodissociation of  $\text{O}_2$  forms two oxygen atoms (reaction 1), and the subsequent recombination of the oxygen atom with  $\text{O}_2$  (reaction 2) is the source of stratospheric  $\text{O}_3$ . A major uncertainty in the study of the evolution of  $\text{O}_3$  is our lack of knowledge concerning the exact chronology for the evolution of  $\text{O}_2$ . For example, Berkner and Marshall (1965) have speculated that  $\text{O}_2$  rose from  $10^{-3}$  of its present atmospheric level (P.A.L.) to its present atmospheric level in the more recent past, over the last 600 million years, whereas Walker (1978) has suggested that  $\text{O}_2$  rose rapidly from essentially zero to within a factor of 10 of its present atmospheric level as early as 2 billion years ago. Due to the uncertainty in the chronology of the evolution of atmospheric  $\text{O}_2$ , the evolution of  $\text{O}_3$  has been studied in terms of the level of  $\text{O}_2$  in units of P.A.L. The first investigation of the evolution of  $\text{O}_3$  in the  $\text{O}_2$ -deficient paleoatmosphere was the qualitative treatment of Berkner and Marshall (1965). Ratner and Walker (1972) studied the evolution of  $\text{O}_3$  in a pure oxygen atmosphere using the four Chapman reactions, but

TABLE I

The variation of ozone column above the surface as function of oxygen level (Levine *et al.*, 1979b)

Oxygen level (P.A.L.)	Ozone column (molec. cm <sup>-2</sup> )
1	1.13 (19)*
10 <sup>-1</sup>	1.59 (19)
10 <sup>-2</sup>	6.74 (18)
10 <sup>-3</sup>	8.71 (17)
10 <sup>-4</sup>	2.36 (16)

\* 1.13 (19) is read as  $1.13 \times 10^{19}$ .

neglected the effects of vertical transport. Vertical transport has been shown to be important in determining the vertical distribution of O<sub>3</sub>, particularly below the peak of the O<sub>3</sub> layer (Nicolet, 1975). Blake and Carver (1977) added nitrogen and hydrogen species chemistry, but again neglected the effects of vertical transport. Next, Levine *et al.* (1979b) studied the evolution of O<sub>3</sub> with a stratospheric photochemical model that included the photochemistry and chemistry of the oxygen, nitrogen, and hydrogen species, and for the first time included the effect of vertical eddy transport on the calculated profiles of the species in the paleoatmosphere. In a companion study, Levine and Boughner (1979) studied the coupling between O<sub>3</sub> and the temperature structure of the paleoatmosphere using a photochemical/radiative-convective temperature model. Katsumori (1979) also studied the coupling of O<sub>3</sub> and temperature structure of the paleoatmosphere using a Chapman scheme photochemical model and a radiative-convective temperature model.

The purpose of this paper is to study how paleoatmospheric levels of oxygen and ozone controlled the solar ultraviolet radiation reaching the surface of the Earth. To perform these calculations which are described in the following section, we need to know how the total ozone column above the surface varied with the level of evolving molecular oxygen. The variation of the total ozone column above the surface as a function of molecular oxygen level, expressed in terms of present atmospheric level (P.A.L.) of oxygen for equinoctial conditions (latitude of 30° and solar declination of 0°), based on the photochemical calculations of Levine *et al.* (1979b), is summarized in Table I. Ratner and Walker (1972) first pointed out that the ozone column maximized for an oxygen level of 10<sup>-1</sup> P.A.L. This feature has since been verified by all photochemical calculations (Blake and Carver, 1977; Levine *et al.*, 1979b; and Katsumori, 1979).

The calculations of O<sub>3</sub> in the O<sub>2</sub>-deficient paleoatmosphere described in Levine *et al.* (1979b) and used in the calculations in this paper were obtained with a stratospheric photochemical model. Several tropospheric chemical, photochemical, and physical processes which may have affected the levels of O<sub>3</sub> in the O<sub>2</sub>-deficient paleoatmosphere

that are not included in the stratospheric photochemical model of Levine *et al.* (1979b) are the inclusion of the surface as a sink for O<sub>3</sub>, the rainout of soluble tropospheric species, and the inclusion of the chemistry of carbon and chlorine species.

#### 4. Solar Ultraviolet Radiation

We have calculated the variation of solar ultraviolet radiation reaching the Earth's surface as O<sub>3</sub> evolved to its present atmospheric level by considering the attenuation of the solar ultraviolet radiation due to the absorption by O<sub>3</sub>, O<sub>2</sub>, H<sub>2</sub>O, CO<sub>2</sub>, and CH<sub>4</sub> using the following form of Beer's Law:

$$I(\lambda, \theta, t) = I(\lambda, \infty) \exp[-\tau(\lambda, z, t)], \quad (12)$$

where  $I(\lambda, \theta, t)$  is the solar ultraviolet radiation reaching the Earth's surface,  $I(\lambda, \infty)$  is the solar ultraviolet radiation incident at the top of the atmosphere,  $\tau(\lambda, t, z)$ , the optical depth for photoabsorption by the various atmospheric constituents above altitude  $z$ , is given by,

$$\tau(\lambda, z, t) = \sum_i N_i(z) \sigma_i(\lambda) \sec \theta(t), \quad (13)$$

where  $N_i$  is the vertical column density above altitude  $z$  of absorber  $i$  whose photoabsorption cross-section is  $\sigma_i(\lambda)$ , and  $\theta$  is the solar zenith angle. The solar zenith angle depends not only on time of day, but also on latitude and season; i.e.,

$$\cos \theta(t) = \cos \omega t \cos L \cos D + \sin L \sin D, \quad (14)$$

where  $L$  is the latitude and  $D$  is the solar declination. All of the calculations of  $I(\lambda, z, t)$  in this paper are diurnal averages for a specified latitude and solar declination based on the computational procedure of Rundel (1977). Values of  $I(\lambda, \infty)$  covering the region of biological significance between 184.6 and 342.5 nm using the solar flux data of Ackerman (1971) were used in this study. The absorption cross-sections for O<sub>3</sub>, O<sub>2</sub>, H<sub>2</sub>O, CO<sub>2</sub>, and CH<sub>4</sub> were folded into these spectral intervals (Levine *et al.*, 1979b). Present atmospheric profiles of H<sub>2</sub>O, CO<sub>2</sub>, and CH<sub>4</sub> were assumed for these calculations.

In the present calculations we are interested in how paleoatmospheric levels of oxygen and ozone controlled the flux of solar ultraviolet radiation reaching the Earth's surface. Therefore, we have only considered the attenuation of the incident solar ultraviolet beam by molecular absorption, and have not included the effects of scattering by molecules and aerosols, clouds, and surface reflectivity. The effect of molecular multiple scattering on incoming solar radiation has been considered by Luther and Gelinias (1976), while Shettle and Green (1974) have studied the effect of aerosols on incoming solar radiation. Luther and Gelinias (1976) calculated the flux ratio of multiple molecular scattering to pure absorption between 200 and 300 nm for selected altitudes in the present atmosphere. Extrapolation of these calculations for the present atmosphere to our calculations for the paleoatmosphere with different levels of ozone and total atmospheric molecules is not easy. However, it appears that the inclusion of multiple molecular scattering may decrease the surface ultraviolet flux between 200 and 300 nm by less than 50%. Shettle

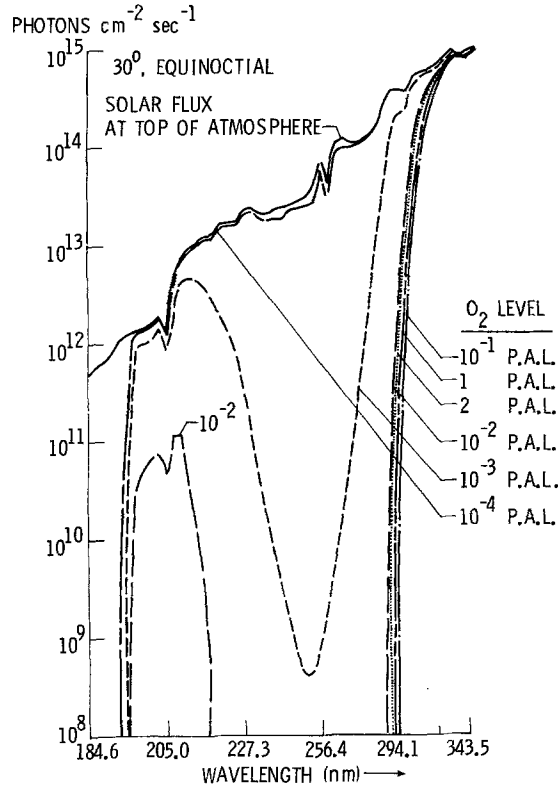


Fig. 1. The solar ultraviolet radiation between 184.6 and 342.5 nm reaching the Earth's surface for O<sub>3</sub> levels corresponding to O<sub>2</sub> levels ranging from 10<sup>-4</sup> to 2 P.A.L. for a latitude of 30° and a solar declination of 0° (equinoctial conditions).

and Green (1974) concluded that by including present atmospheric levels of aerosols, the total (direct and diffuse) ultraviolet flux reaching the Earth's surface will decrease by 10–20%. However, we can only speculate on the levels of aerosols in the paleoatmosphere. Another difficult question to answer is the role played by clouds on the transfer of ultraviolet radiation in the paleoatmosphere. To consider the role of clouds would require knowledge about the chemical composition, optical properties, and distribution of clouds in the paleoatmosphere. Finally, it should be pointed out that some gas or gases abundant in the paleoatmosphere, but missing or deficient in the present atmosphere, may have provided a good ultraviolet screen in the paleoatmosphere.

The solar ultraviolet radiation reaching the Earth's surface was calculated using Equation (12) for O<sub>2</sub> levels ranging from 10<sup>-4</sup> to 1 present atmospheric level (P.A.L.). Calculations were performed for a latitude of 30° for equinoctial conditions (the solar declination equal to 0°) and are summarized in Figure 1 and Table II. In Figure 1 the solar ultraviolet flux at the top of the atmosphere and at the surface in units of photons  $\text{cm}^{-2} \text{s}^{-1}$  between 185.6 and 342.5 nm as a function of O<sub>2</sub> level is plotted. Inspection of Figure 1 shows

TABLE II  
Solar ultraviolet radiation between 200.0–303.0 nm at top of atmosphere and at surface for levels corresponding to various O<sub>2</sub> levels (PAL)  
(for latitude = 30°; solar declination = 0°) (in photons cm<sup>-2</sup> s<sup>-1</sup> and ergs cm<sup>-2</sup> s<sup>-1</sup>)

Spectral interval (nm)	Top of atmosphere	Surface: O <sub>2</sub> = 10 <sup>-4</sup> PAL	Surface: O <sub>2</sub> = 10 <sup>-3</sup> PAL	Surface: O <sub>2</sub> = 10 <sup>-2</sup> PAL	Surface O <sub>2</sub> = 10 <sup>-1</sup> PAL	Surface: O <sub>2</sub> = 1 PAL
200.0–202.0	1.63 × 10 <sup>12</sup> 1.61 × 10 <sup>1</sup>	1.60 × 10 <sup>12</sup> 15.80	1.09 × 10 <sup>12</sup> 10.77	6.30 × 10 <sup>10</sup> .62	4.52 × 10 <sup>6</sup> 4.46 × 10 <sup>-5</sup>	2.45 × 10 <sup>-19</sup> 2.42 × 10 <sup>-30</sup>
202.0–204.1	1.95 × 10 <sup>12</sup> 19.07	1.92 × 10 <sup>12</sup> 18.77	1.30 × 10 <sup>12</sup> 12.71	7.46 × 10 <sup>10</sup> .72	7.31 × 10 <sup>6</sup> 7.15 × 10 <sup>-5</sup>	1.41 × 10 <sup>-17</sup> 1.37 × 10 <sup>-28</sup>
204.1–206.2	1.32 × 10 <sup>12</sup> 12.77	1.30 × 10 <sup>12</sup> 12.58	8.76 × 10 <sup>11</sup> 8.78	4.95 × 10 <sup>10</sup> 4.79 × 10 <sup>-1</sup>	8.86 × 10 <sup>6</sup> 8.57 × 10 <sup>-5</sup>	2.64 × 10 <sup>-14</sup> 2.55 × 10 <sup>-25</sup>
206.2–208.3	4.20 × 10 <sup>12</sup> 4.02 × 10 <sup>1</sup>	4.13 × 10 <sup>12</sup> 3.95 × 10 <sup>1</sup>	2.63 × 10 <sup>12</sup> 2.52 × 10 <sup>1</sup>	1.01 × 10 <sup>11</sup> 9.67 × 10 <sup>-1</sup>	1.21 × 10 <sup>7</sup> 1.15 × 10 <sup>-4</sup>	5.17 × 10 <sup>-13</sup> 4.95 × 10 <sup>-24</sup>
208.3–210.5	7.30 × 10 <sup>12</sup> 6.92 × 10 <sup>1</sup>	7.17 × 10 <sup>12</sup> 6.80 × 10 <sup>1</sup>	4.26 × 10 <sup>12</sup> 4.04 × 10 <sup>1</sup>	1.02 × 10 <sup>11</sup> 9.67 × 10 <sup>-1</sup>	6.97 × 10 <sup>6</sup> 6.61 × 10 <sup>-5</sup>	3.59 × 10 <sup>-12</sup> 3.40 × 10 <sup>-23</sup>
210.5–212.8	9.42 × 10 <sup>12</sup> 8.83 × 10 <sup>1</sup>	9.22 × 10 <sup>12</sup> 8.65 × 10 <sup>1</sup>	4.77 × 10 <sup>12</sup> 4.47 × 10 <sup>1</sup>	4.49 × 10 <sup>10</sup> 4.21 × 10 <sup>-1</sup>	9.12 × 10 <sup>5</sup> 8.55 × 10 <sup>-6</sup>	1.82 × 10 <sup>-11</sup> 1.70 × 10 <sup>-22</sup>
212.8–215.0	1.06 × 10 <sup>13</sup> 9.84 × 10 <sup>1</sup>	1.03 × 10 <sup>13</sup> 9.56 × 10 <sup>1</sup>	4.27 × 10 <sup>12</sup> 3.96 × 10 <sup>1</sup>	8.63 × 10 <sup>8</sup> 8.01 × 10 <sup>-2</sup>	2.06 × 10 <sup>4</sup> 1.91 × 10 <sup>-9</sup>	2.94 × 10 <sup>-11</sup> 2.73 × 10 <sup>-22</sup>
215.0–217.4	1.34 × 10 <sup>13</sup> 1.23 × 10 <sup>2</sup>	1.29 × 10 <sup>13</sup> 1.18 × 10 <sup>2</sup>	3.94 × 10 <sup>12</sup> 3.61 × 10 <sup>1</sup>	9.84 × 10 <sup>8</sup> 9.03 × 10 <sup>-3</sup>	1.18 × 10 <sup>2</sup> 1.08 × 10 <sup>-9</sup>	2.14 × 10 <sup>-11</sup> 1.96 × 10 <sup>-22</sup>
217.4–219.8	1.32 × 10 <sup>13</sup> 1.19 × 10 <sup>2</sup>	1.26 × 10 <sup>13</sup> 1.14 × 10 <sup>2</sup>	2.74 × 10 <sup>12</sup> 2.48 × 10 <sup>1</sup>	6.55 × 10 <sup>7</sup> 5.95 × 10 <sup>-4</sup>	2.65 × 10 <sup>-1</sup> 2.40 × 10 <sup>-12</sup>	7.46 × 10 <sup>-12</sup> 6.77 × 10 <sup>-23</sup>
219.8–222.2	1.73 × 10 <sup>13</sup> 1.55 × 10 <sup>2</sup>	1.63 × 10 <sup>13</sup> 1.46 × 10 <sup>2</sup>	2.28 × 10 <sup>12</sup> 2.04 × 10 <sup>1</sup>	2.65 × 10 <sup>6</sup> 2.38 × 10 <sup>-5</sup>	1.24 × 10 <sup>-4</sup> 1.11 × 10 <sup>-15</sup>	7.63 × 10 <sup>-13</sup> 6.85 × 10 <sup>-24</sup>
222.2–224.7	1.80 × 10 <sup>13</sup> 1.60 × 10 <sup>2</sup>	1.67 × 10 <sup>13</sup> 1.48 × 10 <sup>2</sup>	1.32 × 10 <sup>12</sup> 1.17 × 10 <sup>1</sup>	3.10 × 10 <sup>4</sup> 2.75 × 10 <sup>-7</sup>	4.19 × 10 <sup>-9</sup> 3.72 × 10 <sup>-20</sup>	1.07 × 10 <sup>-14</sup> 9.51 × 10 <sup>-26</sup>
224.7–227.3	1.82 × 10 <sup>13</sup> 1.59 × 10 <sup>2</sup>	1.66 × 10 <sup>13</sup> 1.45 × 10 <sup>2</sup>	6.69 × 10 <sup>11</sup> 5.87 × 10 <sup>0</sup>	1.50 × 10 <sup>2</sup> 1.31 × 10 <sup>-4</sup>	1.81 × 10 <sup>-14</sup> 1.59 × 10 <sup>-25</sup>	3.32 × 10 <sup>-17</sup> 2.91 × 10 <sup>-28</sup>

Table II (continued)

Spectral Interval (nm)	Top of atmosphere	Surface:			Surface:			Surface:		
		$O_2 = 10^{-4}$ PAL	$O_2 = 10^{-3}$ PAL	$O_2 = 10^{-2}$ PAL	$O_2 = 10^{-1}$ PAL	$O_2 = 10^{-2}$ PAL	$O_2 = 10^{-1}$ PAL	$O_2 = 1$ PAL		
227.3-229.9	$2.26 \times 10^{13}$ $1.96 \times 10^2$	$2.02 \times 10^{13}$ $1.75 \times 10^2$	$3.86 \times 10^{11}$ $3.35 \times 10^0$	$5.10 \times 10^{-1}$ $4.43 \times 10^{-1.2}$	$2.67 \times 10^{-2.0}$ $2.32 \times 10^{-3.1}$	$5.32 \times 10^{-2.0}$ $4.62 \times 10^{-3.1}$				
229.9-232.6	$2.40 \times 10^{13}$ $2.06 \times 10^2$	$2.10 \times 10^{13}$ $1.80 \times 10^2$	$1.78 \times 10^{11}$ $1.52 \times 10^0$	$8.64 \times 10^{-4}$ $7.42 \times 10^{-1.5}$	$9.36 \times 10^{-2.7}$ $8.03 \times 10^{-3.8}$	$3.08 \times 10^{-2.3}$ $2.64 \times 10^{-3.4}$				
232.6-235.3	$2.25 \times 10^{13}$ $1.91 \times 10^2$	$1.91 \times 10^{13}$ $1.62 \times 10^2$	$6.33 \times 10^{10}$ $5.37 \times 10^{-1}$	$4.70 \times 10^{-7}$ $3.99 \times 10^{-1.8}$	$2.69 \times 10^{-3.4}$ $2.28 \times 10^{-4.5}$	$3.36 \times 10^{-2.7}$ $2.85 \times 10^{-3.8}$				
235.3-238.1	$2.21 \times 10^{13}$ $1.85 \times 10^2$	$1.83 \times 10^{13}$ $1.53 \times 10^2$	$2.11 \times 10^{10}$ $1.77 \times 10^{-1}$	$1.14 \times 10^{-1.0}$ $9.56 \times 10^{-2.2}$	$1.06 \times 10^{-4.2}$ $8.89 \times 10^{-5.4}$	$8.23 \times 10^{-3.2}$ $6.90 \times 10^{-4.3}$				
238.1-241.0	$2.32 \times 10^{13}$ $1.92 \times 10^2$	$1.86 \times 10^{13}$ $1.54 \times 10^2$	$7.24 \times 10^9$ $6.00 \times 10^{-2}$	$2.15 \times 10^{-1.4}$ $1.78 \times 10^{-2.5}$	$2.20 \times 10^{-5.1}$ $1.82 \times 10^{-6.2}$	$1.57 \times 10^{-3.7}$ $1.30 \times 10^{-4.8}$				
241.0-243.9	$2.50 \times 10^{13}$ $2.04 \times 10^2$	$1.95 \times 10^{13}$ $1.59 \times 10^2$	$2.77 \times 10^9$ $2.26 \times 10^{-2}$	$7.96 \times 10^{-1.8}$ $6.52 \times 10^{-2.9}$	$2.48 \times 10^{-5.9}$ $2.03 \times 10^{-7.0}$	$6.53 \times 10^{-4.0}$ $5.34 \times 10^{-5.1}$				
243.9-246.9	$2.73 \times 10^{13}$ $2.20 \times 10^2$	$2.07 \times 10^{13}$ $1.67 \times 10^2$	$1.10 \times 10^9$ $8.90 \times 10^{-3}$	$3.69 \times 10^{-2.1}$ $2.98 \times 10^{-3.2}$	$4.00 \times 10^{-6.7}$ $3.23 \times 10^{-7.8}$	$5.03 \times 10^{-4.4}$ $4.07 \times 10^{-5.5}$				
246.9-250.0	$2.88 \times 10^{13}$ $2.30 \times 10^2$	$2.14 \times 10^{13}$ $1.71 \times 10^2$	$5.73 \times 10^8$ $4.58 \times 10^{-3}$	$1.66 \times 10^{-2.5}$ $1.32 \times 10^{-3.4}$	$1.09 \times 10^{-7.2}$ $8.71 \times 10^{-8.4}$	$5.67 \times 10^{-4.8}$ $4.53 \times 10^{-5.9}$				
250.0-253.2	$3.02 \times 10^{13}$ $2.38 \times 10^2$	$2.22 \times 10^{13}$ $1.75 \times 10^2$	$4.01 \times 10^8$ $3.16 \times 10^{-3}$	$7.69 \times 10^{-2.5}$ $6.07 \times 10^{-3.6}$	$7.31 \times 10^{-7.6}$ $5.77 \times 10^{-8.7}$	$3.20 \times 10^{-5.0}$ $2.52 \times 10^{-6.1}$				
253.2-256.4	$3.97 \times 10^{13}$ $3.09 \times 10^2$	$2.91 \times 10^{13}$ $2.26 \times 10^2$	$4.76 \times 10^8$ $3.71 \times 10^{-3}$	$4.63 \times 10^{-2.5}$ $3.60 \times 10^{-3.6}$	$1.53 \times 10^{-7.6}$ $1.19 \times 10^{-8.7}$	$1.14 \times 10^{-5.0}$ $8.88 \times 10^{-6.2}$				
256.4-259.7	$7.13 \times 10^{13}$ $5.48 \times 10^2$	$5.25 \times 10^{13}$ $4.04 \times 10^2$	$9.46 \times 10^8$ $7.28 \times 10^{-3}$	$1.81 \times 10^{-2.4}$ $1.39 \times 10^{-3.5}$	$1.72 \times 10^{-7.5}$ $1.32 \times 10^{-8.6}$	$7.55 \times 10^{-5.0}$ $5.81 \times 10^{-6.1}$				

Table II (continued)

Spectral Interval (nm)	Top of atmosphere	Surface: $O_2 = 10^{-4}$ PAL	Surface: $O_2 = 10^{-3}$ PAL	Surface: $O_2 = 10^{-2}$ PAL	Surface: $O_2 = 10^{-1}$ PAL	Surface: $O_2 = 1$ PAL
259.7–263.2	$4.37 \times 10^{13}$ $3.31 \times 10^2$	$3.29 \times 10^{13}$ $2.49 \times 10^2$	$1.30 \times 10^9$ $9.87 \times 10^{-3}$	$5.70 \times 10^{-2}$ $4.33 \times 10^{-3}$	$2.58 \times 10^{-6}$ $1.96 \times 10^{-8}$	$1.60 \times 10^{-4}$ $1.21 \times 10^{-6}$
263.2–266.7	$1.12 \times 10^{14}$ $8.39 \times 10^2$	$8.63 \times 10^{13}$ $6.46 \times 10^2$	$8.05 \times 10^9$ $6.03 \times 10^{-2}$	$1.29 \times 10^{-1}$ $9.67 \times 10^{-3}$	$5.83 \times 10^{-2}$ $4.37 \times 10^{-3}$	$3.54 \times 10^{-4}$ $2.65 \times 10^{-5}$
266.7–270.3	$1.25 \times 10^{14}$ $9.24 \times 10^2$	$9.96 \times 10^{13}$ $7.36 \times 10^2$	$3.02 \times 10^{10}$ $2.23 \times 10^{-1}$	$1.67 \times 10^{-1}$ $1.23 \times 10^{-2}$	$2.47 \times 10^{-3}$ $1.82 \times 10^{-6}$	$2.54 \times 10^{-2}$ $1.87 \times 10^{-4}$
270.3–274.0	$1.16 \times 10^{14}$ $8.46 \times 10^2$	$9.61 \times 10^{13}$ $7.01 \times 10^2$	$1.18 \times 10^{11}$ $8.61 \times 10^{-1}$	$1.00 \times 10^{-9}$ $7.29 \times 10^{-2}$	$4.98 \times 10^{-4}$ $3.63 \times 10^{-2}$	$2.68 \times 10^{-2}$ $1.95 \times 10^{-3}$
274.0–277.8	$1.19 \times 10^{14}$ $8.56 \times 10^2$	$1.03 \times 10^{14}$ $7.41 \times 10^2$	$5.53 \times 10^{11}$ $3.98$	$1.23 \times 10^{-4}$ $8.85 \times 10^{-1}$	$4.83 \times 10^{-2}$ $3.47 \times 10^{-4}$	$8.90 \times 10^{-1}$ $6.40 \times 10^{-2}$
277.8–281.7	$1.38 \times 10^{14}$ $9.79 \times 10^2$	$1.24 \times 10^{14}$ $8.80 \times 10^2$	$2.44 \times 10^{12}$ $1.73 \times 10^1$	$4.23 \times 10^0$ $3.00 \times 10^{-1}$	$1.93 \times 10^{-1}$ $1.37 \times 10^{-2}$	$3.18 \times 10^{-9}$ $2.25 \times 10^{-2}$
281.7–285.7	$1.70 \times 10^{14}$ $1.19 \times 10^3$	$1.57 \times 10^{14}$ $1.09 \times 10^3$	$9.61 \times 10^{12}$ $6.72 \times 10^1$	$4.09 \times 10^4$ $2.86 \times 10^{-7}$	$3.61 \times 10^{-9}$ $2.52 \times 10^{-2}$	$1.31 \times 10^{-2}$ $9.17 \times 10^{-14}$
285.7–289.9	$2.46 \times 10^{14}$ $1.69 \times 10^3$	$2.33 \times 10^{14}$ $1.60 \times 10^3$	$3.53 \times 10^{13}$ $2.43 \times 10^2$	$7.73 \times 10^7$ $5.33 \times 10^{-4}$	$1.15 \times 10^{-1}$ $7.93 \times 10^{-1}$	$3.15 \times 10^3$ $2.17 \times 10^{-8}$
298.9–294.1	$3.90 \times 10^{14}$ $2.65 \times 10^3$	$3.78 \times 10^{14}$ $2.57 \times 10^3$	$1.23 \times 10^{14}$ $8.36 \times 10^2$	$5.37 \times 10^{10}$ $3.65 \times 10^{-1}$	$3.09 \times 10^5$ $2.10 \times 10^{-6}$	$1.33 \times 10^8$ $9.04 \times 10^{-4}$
294.1–298.5	$3.99 \times 10^{14}$ $2.67 \times 10^3$	$3.92 \times 10^{14}$ $2.62 \times 10^3$	$2.04 \times 10^{14}$ $1.36 \times 10^3$	$2.32 \times 10^{12}$ $1.55 \times 10^1$	$2.15 \times 10^9$ $1.44 \times 10^{-2}$	$7.19 \times 10^{10}$ $4.81 \times 10^{-1}$
298.5–303.0	$3.86 \times 10^{14}$ $2.54 \times 10^3$	$3.82 \times 10^{14}$ $2.52 \times 10^3$	$2.66 \times 10^{14}$ $1.75 \times 10^3$	$2.17 \times 10^{13}$ $1.43 \times 10^2$	$4.37 \times 10^{11}$ $2.88$	$3.11 \times 10^{12}$ $2.05 \times 10^1$

the existence of an 'atmospheric window' between about 195 and 215 nm. Solar radiation shortward of 195 nm is absorbed by O<sub>2</sub>, and radiation longward of 215 nm is absorbed by O<sub>3</sub>. In Table II these calculations in units of both photons cm<sup>-2</sup> s<sup>-1</sup> and ergs cm<sup>-2</sup> s<sup>-1</sup> for each of the 34 spectral intervals between 200.0 and 303.0 nm as a function of O<sub>2</sub> level are presented.

The question of what level of surface ultraviolet radiation, if any, is lethal to biological systems is extremely difficult to answer. The maximum tolerable limit of ultraviolet radiation depends on both the intensity and the spectral interval considered, since the absorption cross section of O<sub>3</sub> and the intensity of the solar flux vary significantly between 200 and 300 nm. For example, inspection of Table II indicates that the maximum surface intensity occurs at the beginning and end of the spectral interval under consideration, i.e., at 200 and 300 nm. The minimum surface intensity occurs at about 250 nm. For an O<sub>2</sub> level of 10<sup>-3</sup> P.A.L., the surface intensity varies by six orders of magnitude from 10<sup>14</sup> photons cm<sup>-2</sup> s<sup>-1</sup> at 298.5 nm to 10<sup>8</sup> photons cm<sup>-2</sup> s<sup>-1</sup> at 250.0 nm. For an O<sub>2</sub> level of 10<sup>-2</sup> P.A.L., the surface intensity varies by some 38 orders of magnitude from 10<sup>13</sup> photons cm<sup>-2</sup> s<sup>-1</sup> at 298.5 nm to 10<sup>-2.5</sup> photons cm<sup>-2</sup> s<sup>-1</sup> at 253.2 nm. For an O<sub>2</sub> level of 10<sup>-1</sup> P.A.L., O<sub>2</sub> and O<sub>3</sub> effectively shield the surface from solar radiation between 200 and 300 nm.

While the role of enhanced levels of surface ultraviolet radiation on biological systems and biological evolution must be left to the biologists, we can comment on several atmospheric aspects of this investigation. The values of surface ultraviolet radiation calculated in this study and tabulated in Table II may represent upper limit values. It is possible that some minor gas in the paleoatmosphere, such as sulfur dioxide, may have provided an efficient ultraviolet screen. Perhaps increased volcanic activity during the early history of the Earth resulted in greatly enhanced levels of atmospheric aerosols and a more turbid atmosphere, which would result in increased attenuation of the ultraviolet radiation reaching the Earth's surface. Increased atmospheric turbidity can have a significant effect on the distribution of solar radiation reaching a planetary surface (Levine *et al.*, 1977). As pointed out earlier, the role of paleoatmospheric clouds on the transfer of ultraviolet radiation is a major deficiency in our understanding. We do not know the chemical composition, optical properties, or the extent and distribution of the clouds in the paleoatmosphere. The length of the day, the latitude, and solar declination all determine the intensity of the solar ultraviolet radiation that an organism at the surface receives. The latitude and solar declination which determine the solar zenith angle and the atmospheric mass length for the transfer of radiation have a major effect on the level of solar ultraviolet radiation reaching the surface (Levine *et al.*, 1980). There are indications that the rotation period of the early Earth was significantly shorter than the present period of 24 hr. Finally, the role of surface ultraviolet radiation on the origin and evolution of life on Earth must wait until we have a more precise chronology for the evolution of atmospheric O<sub>2</sub>.

## References

- Ackermann, M.: 1971, *Mesospheric Models and Related Experiments*, D. Reidel Publ. Co., Dordrecht, Holland, p. 149.
- Bates, D. R. and Nicolet, M.: 1950, *J. Geophys. Res.* **55**, 301.
- Berkner, L. V. and Marshall, L. C.: 1965, *J. Atmos. Sci.* **22**, 225.
- Blake, A. J. and Carver, J. H.: 1977, *J. Atmos. Sci.* **34**, 720.
- Brinkmann, R. T.: 1969, *J. Geophys. Res.* **74**, 5355.
- Chapman, S.: 1930, *Mem. Roy. Meteor. Soc.* **3**, 103.
- Crutzen, P. J.: 1970, *Quart. J. Roy. Meteor. Soc.* **96**, 320.
- Crutzen, P. J.: 1971, *J. Geophys. Res.* **76**, 7311.
- Hart, M. H.: 1970, *Icarus* **33**, 23.
- Johnston, H. S.: 1971, *Science* **173**, 517.
- Johnston, H. S.: 1975, *Rev. Geophys. Space Phys.* **13**, 637.
- Levine, J. S. and Boughner, R. E.: 1979, *Icarus* **39**, 310.
- Levine, J. S., Kraemer, D. R., and Kuhn, W. R.: 1977, *Icarus* **31**, 136.
- Levine, J. S., Hughes, R. E., Chameides, W. L., and Howell, W. E.: 1979a, *Geophys. Res. Letters* **6**, 557.
- Levine, J. S., Hays, P. B., and Walker, J. C. G.: 1979b, *Icarus* **39**, 295.
- Levine, J. S., Boughner, R. E., and Smith, K. A.: 1980, *Origins of Life* **10**, 199; also reprinted in *Limits of life*, edited by C. Ponnampertuma and L. Margulis, D. Reidel Publ. Co., Dordrecht, 1980, pp. 105–119.
- Luther, F. M. and Gelinas, R. J.: 1976, *J. Geophys. Res.* **81**, 1125.
- Margulis, L., Walker, J. C. G., and Rambler, M.: 1976, *Nature* **264**, 620.
- Nicolet, M.: 1975, *Rev. Geophys. Space Phys.* **13**, 593.
- Rambler, M., Margulis, L., and Barghoorn, E. S.: 1976, *Chemical Evolution and the Precambrian*, Academic Press, New York, p. 133.
- Ratner, M. I. and Walker, J. C. G.: 1972, *J. Atmos. Sci.* **29**, 803.
- Rundel, D. R.: 1977, *J. Atmos. Sci.* **34**, 639.
- Sagan, C.: 1973, *J. Theor. Biol.* **39**, 195.
- Shettle, E. P. and Green A. E. S.: 1974, *Appl. Optics* **13**, 1567.
- Towe, K. M.: 1978, *Nature* **274**, 657.
- Walker, J. C. G.: 1977, *Evolution of the Atmosphere*, MacMillan, New York.
- Walker, J. C. G.: 1978, *Pure Appl. Geophys.* **117**, 498.